Monolysocardiolipins accumulate in Barth syndrome but do not lead to enhanced apoptosis

Fredoen Valianpour,* Voula Mitsakos,† Dimitri Schlemmer,§ Jeffrey A. Towbin, Juliet M. Taylor,† Paul G. Ekert,†† David R. Thorburn,† Arnold Munnich,§ Ronald J. A. Wanders,* Peter G. Barth,* and Frédéric M. Vaz[1,]***

Laboratory of Genetic Metabolic Diseases,* Departments of Clinical Chemistry and Pediatrics, Emma Children's Hospital, Academic Medical Center, University of Amsterdam, 1100 DE Amsterdam, The Netherlands; Murdoch Childrens Research Institute,† Royal Children's Hospital and Department of Paediatrics, University of Melbourne, Melbourne, Victoria 3052, Australia; Hopital Necker Enfants Malades,§ Department of Genetics and Institut National de la Santé et de la Recherche Médicale U-393, 75743 Paris, Cedex 15, France; Baylor College of Medicine and Texas Children's Hospital,** Department of Pediatrics (Cardiology), Houston, TX; and the Walter and Eliza Hall Institute of Medical Research, the Murdoch Childrens Research Institute, and Department of Neonatology,†† Royal Children's Hospital, Melbourne, Victoria 3052, Australia

Abstract Barth syndrome (BTHS) is an X-linked recessive disorder that is biochemically characterized by low cellular levels of the mitochondrial phospholipid cardiolipin (CL). Previously, we discovered that the yeast disruptant of the *TAZ* ortholog in *Saccharomyces cerevisiae* not only displays CL deficiency but also accumulates monolysocardiolipins (MLCLs), which are intermediates in CL remodeling. Therefore, we set out to investigate whether MLCL accumulation also occurs in BTHS. Indeed, we observed MLCL accumulation in heart, muscle, lymphocytes, and cultured lymphoblasts of BTHS patients; however, only very low levels of these lysophospholipids were found in platelets and fibroblasts of these patients. Although the fatty acid composition of the MLCLs was different depending on the tissue source, it did parallel the fatty acid composition of the (remaining) CLs. The possible implications of these findings for the two reported CL remodeling mechanisms, transacylation and deacylation/reacylation, are discussed. Because MLCLs have been proposed to be involved in the initiation of apoptosome-mediated cell death by the sequestration of the proapoptotic protein (t)BH3-interacting domain death agonist (Bid) to the mitochondrial membrane, we used control and BTHS lymphoblasts to investigate whether the accumulation of MLCLs results in higher levels of apoptosis. We found no differences in susceptibility to death receptor-mediated apoptosis or in cellular distribution of Bid, cytochrome *c*, and other parameters, implying that MLCL accumulation does not lead to enhanced apoptosis in cultured BTHS lymphoblasts.— Valianpour, F., V. Mitsakos, D. Schlemmer, J. A. Towbin, J. M. Taylor, P. G. Ekert, D. R. Thorburn, A. Munnich, R. J. A. Wanders, P. G. Barth, and F. M. Vaz. **Monolysocardiolipins accumulate in Barth syndrome but do not lead to enhanced apoptosis. *J. Lipid Res.* 2005.** 46: **1182–1195.**

Supplementary key words cardiolipin • tafazzin • lymphoblasts

Manuscript received 14 February 2005 and in revised form 23 March 2005.

Published, JLR Papers in Press, April 1, 2005.
DOI 10.1194/jlr.M500056-JLR200

Barth syndrome [BTHS; Mendelian Inheritance in Man (MIM) 302060] is an X-linked recessive disorder that clinically is characterized by cardiomyopathy, skeletal myopathy, growth retardation, and neutropenia (1). Additional laboratory findings include intermittent lactic acidemia, low blood cholesterol, and increased urinary excretion of 3-methylglutaconic acid, 3-methylglutaric acid, and 2-ethylhydracrylic acid (2). Moreover, mitochondria of BTHS patients have an abnormal ultrastructure, and several different respiratory chain defects in muscle and fibroblasts have been reported (3, 4). The disease can be fatal in childhood, as a result of cardiac failure or sepsis. The clinical expression of the disease, however, is quite variable in severity and may show profound intrafamilial variability.

Mutations in the *TAZ* gene, which is located at Xq28, are responsible for BTHS (5). Because of the homology of the predicted *TAZ* gene product(s) with acyltransferases involved in phospholipid metabolism, it is suggested that *TAZ* is involved in the remodeling of phospholipids (6). This suggestion was supported by our finding that the incorporation of linoleic acid into cardiolipin (CL) was defective in patients with BTHS, even though their biosynthetic capacity to synthesize CL was entirely normal (7). Additionally, the CL levels have been shown to be markedly decreased in platelets (8), fibroblasts (9), and tissues (10, 11) of patients with BTHS.

CL is a unique polyglycerophospholipid that has a dimeric structure consisting of two phosphatidyl moieties linked

Abbreviations: Bid, BH3-interacting domain death agonist; BTHS, Barth syndrome; CL, cardiolipin; FasL, Fas ligand; I.S., internal standard; MLCL, monolysocardiolipin; PARP, poly (ADP-ribose) polymerase; PC, phosphatidylcholine; PE, phosphatidylethanolamine.

[1] To whom correspondence should be addressed.
e-mail: f.m.vaz@amc.uva.nl

by a glycerol bridge. Therefore, CL has four fatty acyl side chains and two negatively charged phosphate groups. CL is found almost exclusively in the inner mitochondrial membrane and plays a central role in mitochondrial function, especially oxidative phosphorylation, because a number of the respiratory chain complexes and several metabolite transporters require CL for optimal function (12, 13). CL is found throughout nature in mitochondria of animals, plants, and fungi and is a component of bacterial membranes (12). In eukaryotes, CL is synthesized from phosphatidylglycerol and cytidine-5′-diphosphate-1,2-diacyl-*sn*-glycerol in a reaction catalyzed by CL synthase. In animal tissues, especially in heart and muscle, CL contains almost exclusively C18 fatty acids, and 80% of this is typically linoleic acid, C18:2(n-6) (14, 15). Because CL molecular species produced by CL synthase do not have the proper fatty acid side chains, CL is remodeled to produce the required acyl composition (12–14). The proposed pathway for the remodeling of CL is a deacylation/reacylation mechanism that involves the formation of the intermediate monolysocardiolipin (MLCL) by the action of phospholipase(s) and the reacylation of this compound by one or more acyltransferase(s) (16, 17). Therefore, it has been suggested that the *TAZ* gene encodes an acyltransferase involved in the remodeling of CL. If so, one would expect that the intermediates of remodeling (i.e., MLCLs) would accumulate in BTHS. Recently, we and others have reported that a strain of *Saccharomyces cerevisiae* in which the yeast ortholog of the *TAZ* gene, YPR140w, has been disrupted not only displays CL deficiency but also accumulates MLCLs (18, 19). We showed that the levels of both CL and MLCL normalized after transformation of the disruptant with human tafazzin (19), confirming the direct involvement of *TAZ* in the remodeling of CL. Until now, however, MLCL accumulation has not been observed in cells or tissues from BTHS patients. To investigate whether MLCLs also accumulate in BTHS, we adapted our recently developed method for the measurement of CL (8) to measure CLs, MLCLs, and other phospholipids in cells and tissues. We also investigated how TAZ deficiency affects other phospholipids in these tissues.

Our results show that in addition to CL deficiency in BTHS tissues/cells, there are also abnormalities in other phospholipid classes. Additionally, there is a clear accumulation of MLCLs in muscle, heart, lymphoblasts, and lymphocytes, but surprisingly, only minor increases of these metabolites are observed in fibroblasts and platelets. Because recent research indicates that MLCLs are proapoptotic lipids, we determined whether the MLCL accumulation leads to enhanced apoptosis in BTHS. Our investigations indicate that MLCLs do not lead to enhanced apoptosis in cultured BTHS cells.

MATERIALS AND METHODS

Materials

All solutions were of analytical quality and were purchased from Merck (Darmstadt, Germany). The $(14:0)_4$-CL internal standard (I.S.) and MLCL were purchased from Avanti Polar Lipids (Alabaster, AL). An analytical HPLC LiChrospher Si 60 column (2 × 250 mm, 5 μm particle size) was purchased from Merck.

Cell culture and tissues

Lymphoblasts and Jurkat cells were cultured in RPMI medium containing 10% fetal calf serum, 25 mM HEPES, and 1% penicillin/streptomycin. Cells were collected by centrifugation at 1,500 rpm for 5 min and washed with PBS. Fibroblasts were cultured as described by Valianpour et al. (9). Pellets were used for analysis either directly or were kept frozen at −80°C before analysis. All blood/tissue samples were collected according to institutional guidelines for blood/tissue sampling, including procurement of informed consent of the persons involved or their representatives.

Lipid extraction from cultured cells

Cell pellets were suspended in 300 μl of distilled water and sonicated on ice, 2 × 10 s at 8 W, using a probe-tip vibra-cell sonicater (Sonics and Materials, Danbury, CT). Of this cell suspension, 10 μl was used for protein measurement. I.S. was added to the remaining homogenate [50 μl of a 7.8 μmol/l solution of $(14:0)_4$-CL in 2:1 chloroform-methanol (v/v)] followed by 3 ml of 1:1 chloroform-methanol (v/v). This mixture was shaken vigorously and placed on ice for 15 min, after which it was centrifuged at 1,000 *g* for 5 min. The organic layer was transferred into another tube, and the protein pellet was extracted with 3 ml of 2:1 chloroform-methanol (v/v). The combined organic layers were evaporated under a stream of nitrogen at 50°C. The residue was dissolved in 150 μl of 50:45:5 chloroform-methanol-water (v/v/v), and 5 μl of this solution was injected into the HPLC-tandem MS system.

Lipid extraction from tissues

Approximately 2 mg of cardiac or muscle tissue was placed in a 1.5 ml Eppendorf vial, and its exact wet weight was determined using a microbalance. The Eppendorf vial already contained the I.S., 150 μl of a 7.8 μmol/l solution of $(14:0)_4$-CL in 2:1 chloroform-methanol (v/v) (1,170 pmol), which had been evaporated under a stream of nitrogen at 50°C. The tissue samples were freeze-dried overnight in a benchtop lyophilization system (LabConco, Kansas City, MO). The lyophilized tissues were kept on ice and ground to powder using an Eppendorf micropestle. Three hundred microliters of 1:1 chloroform:methanol (v/v) was added to the tissue powder, and this suspension was sonicated twice for 10 s at 2.5 W. Three milliliters of 1:1 chloroform-methanol (v/v) was added, and this suspension was shaken vigorously, placed on ice for 15 min, and centrifuged for 5 min at 1,000 *g*. The organic layer was transferred into another tube, and the protein pellet was extracted with 3 ml of 2:1 chloroform-methanol (v/v). The combined organic layers were evaporated under a stream of nitrogen at 50°C. The residue was dissolved in 250 μl of 50:45:5 chloroform-methanol-water (v/v/v), and 5 μl of this solution was injected into the HPLC-tandem MS system.

HPLC

The HPLC system consisted of an HP1100 series binary gradient pump, a vacuum degasser, and a column temperature controller (all from Hewlett-Packard, Wilmington, DE) and a Gilson 231 XL autosampler (Gilson, Villiers-le-Bel, France). The column temperature was maintained at 22°C. The lipid extract was injected onto a 2.1 × 250 mm silica column, 5 μm particle diameter (Merck). The phospholipids were separated from interfering compounds by a linear gradient between solution B (chloroform-methanol, 98:2, v/v) and solution A (methanol-water, 9:1, v/v). Both solutions contained 0.1 ml of 250 ml/l aqueous ammonia (e.g., 25%) per liter of eluent. The gradient (0.3 ml/min)

was as follows: 0–3 min, 20% A to 100% A; 3–8 min, 100% A; 8–8.1 min, 100% A to 0% A; and 8.1–16 min, equilibration with 0% A. All gradient steps were linear, and the total analysis time, including the equilibration, was 16 min. A splitter between the HPLC column and the mass spectrometer was used, and 30 μl/min eluent was introduced into the mass spectrometer.

Mass spectrometry

A Quattro II triple-quadrupole mass spectrometer (Micromass, Manchester, UK) was used in the negative electrospray ionization mode. Nitrogen was used as nebulizing gas. Argon was used as collision gas at a pressure of 2.5×10^{-3} mBar. The capillary voltage used was 3 kV. The source temperature was set at 80°C. Optimal cone voltage energy for MLCLs and CLs was 30 V. Mass spectra of CL and MLCL molecular species were obtained by continuous scanning from 400 to 1,000 *m/z* with a scan rate of 200 Da/s in a time window of 2.5 min, during which both types of compound elute from the column. Daughter fragments of CL and MLCL molecular species were obtained using optimal collision energy of 40 eV as described previously (8). Phosphatidylcholine (PC) molecular species were measured using a parent ion scan (from *m/z* 400 to 1,000) for *m/z* 184.1 in the positive ion mode. Phosphatidylethanolamine (PE) molecular species were measured in the positive ion mode using a neutral loss scan (from *m/z* 400 to 1,000) of the mass 141.1.

In a separate analysis using the same extracts, single-ion recording was used to perform a semiquantitative determination of selected MLCLs and CLs. The area of each (ML)CL peak [$A_{(ML)CL}$] and that of the added I.S. (A_{IS}) was quantified using MassLynx 3.3 (Micromass). If appropriate, the peak areas were corrected for the contribution of naturally occurring isotopes. To compare individual samples, the ratio $A_{(ML)CL}/A_{IS}$ was also corrected for the protein content in case of cell homogenates or wet tissue weight for tissue samples. Because the method is not validated for the different (ML)CL molecular species and because we did not determine whether the response of the I.S. was equal to that of the quantified (ML)CLs, we show these values as arbitrary units, normalized per milligram of tissue or protein content.

Validation

The linear response and detection limit for $(18:2)_3$-MLCL were established by injection of calibration mixtures with different concentrations of this analyte and a constant concentration of $(14:0)_4$-CL as the I.S. The extraction efficiencies for both the I.S. and analytes were obtained by comparing their peak intensities in the extracted calibration mixtures with those in the unextracted calibration mixtures with the same final concentrations without extraction. The intra-assay (within-day) variation of the method was determined by measuring 10 times a nonenriched sample and a sample enriched with commercially available $(18:2)_3$-MLCL at low (2 nmol/mg protein) and high (100 nmol/mg protein) concentrations. The interassay (between-day) variation was determined by measuring blank samples and samples enriched with $(18:2)_3$-MLCL (10 and 100 nmol/mg protein) over 3 weeks. The recovery of the method was established by measuring 10 different samples before and after enrichment with a known amount of $(18:2)_3$-MLCL. We investigated ion suppression from interfering substances by comparison of the peak intensities of both $(18:2)_4$-CL and $(14:0)_4$-CL in the enriched samples with those of calibrator solutions with similar concentrations.

Subcellular fractionation of lymphoblasts and immunoblotting

Control and BTHS lymphoblastoid cells (lymphoblasts) were harvested by centrifugation at 500 *g* and washed twice with phosphate-buffered saline. Cells were resuspended in homogenization buffer (10 mM MOPS buffer containing 250 mM sucrose, 1 mM EGTA, and 2 mM KCl, pH 7.4) and homogenized by five passages through a cell cracker (EMBL, Heidelberg, Germany). The postnuclear supernatant was obtained after centrifuging the homogenate for 10 min at 800 *g* at 4°C, and protein concentration was determined using Bio-Rad Protein Reagent (Hercules, CA). The postnuclear supernatant was centrifuged for 60 min at 100,000 *g* to separate the organelles from the cytosol. The supernatant (cytosol) was collected, and the organelle fraction was washed twice with homogenization buffer. Finally, the organelle pellet was resuspended in an equal volume as that of the cytosol.

Equal aliquots of the organelle and cytosolic fractions, corresponding to 75 μg of the postnuclear supernatant protein, were separated by SDS-PAGE and blotted onto a nitrocellulose membrane using a semidry electroblotting apparatus, and immunoblot analysis was performed as described previously (20).

For the analysis of cleavage of poly (ADP-ribose) polymerase (PARP), lymphoblasts were harvested by centrifugation, washed with phosphate-buffered saline, and lysed by sonication in homogenization buffer. The protein concentration of the homogenate was determined, and 75 μg of protein was loaded on a 10% SDS-PAGE gel.

For the analysis of tBH3-interacting domain death agonist (Bid) binding, mitochondrial fractions (1 mg/ml) from control and BTHS lymphoblastoid cells were incubated with 1 μg/ml tBid (caspase-8-cleaved recombinant human protein; Oncogene Research Products, San Diego, CA) at 30°C for 1 h in 5 mM HEPES, 210 mM mannitol, 70 mM sucrose, 5 mM succinate, 1 mM EGTA, and 0.1 mM PMSF, pH 7.2. After centrifugation at 10,000 *g* for 10 min, mitochondrial pellets were resuspended in phosphate-buffered saline, and 50 μg of protein was loaded on a 15% SDS-PAGE gel.

The following antibodies were used for immunoblotting: anti-Bid (1:2,000; Cell Signaling Technology, Beverly, MA), anti-cytochrome *c* (clone 7H8.2C12, 1:100; Pharmingen, San Diego, CA), anti-PARP (1:1,000; Biomol, Plymouth Meeting, PA), anti-caspase-8 (clone 12F5, 1:2,000; Alexis, Bingham, Nottingham, UK), and anti-porin (Calbiochem, Kilsyth, Victoria, Australia).

Fas ligand induction of cell death

Supernatant from the Neuro2A-CD95L cell line, containing active membrane-bound Fas ligand (FasL), was generated as described previously (21), as was supernatant from Neuro2A cells transfected with an empty vector (Neuro2A-neo). Lymphoblast and Jurkat cells (~1×10^6 cells) were resuspended in FasL supernatant plus various amounts of fresh medium to achieve different FasL dilutions and incubated for 24 h before analysis of cell viability by flow cytometry. Caspase-8 activation was assessed after FasL treatment by washing cells once in phosphate-buffered saline, performing a cell count on resuspended cells, and pelleting an aliquot of ~5×10^6 cells. Cell pellets were resuspended in 50 μl of phosphate-buffered saline and lysed directly in 50 μl of SDS loading buffer, and an aliquot equivalent to 5×10^5 cells was subjected to SDS-PAGE and immunoblotting. Bid cleavage in FasL-treated cells was assessed by immunoblotting of cytosolic and membrane fractions prepared by digitonin fractionation, as described previously (22). Sample loadings were equivalent to 7×10^5 cells in each lane.

RESULTS

Validation

Because MLCLs are present in the yeast model for BTHS (18, 19), we set out to investigate whether these lysophos-

pholipids also accumulate in cells and tissues of BTHS patients. We first adapted our recently developed method to measure CL to enable the detection of MLCLs and validated this method. The main change in our method is the use of a one-phase extraction to increase the recovery of MLCLs. This change did not influence the recovery of CL and that of other phospholipids. Individual MLCL molecular species were measured by scanning negatively charged ions after separation by normal-phase HPLC. The response of the detector was linear to increasing concentrations of commercially available $(18:2)_3$-MLCL at least up to 168 nmol/mg protein ($r^2 = 0.993$). The recovery of the method was 68.2 ± 4.9% at low-level and 78.2 ± 2.2% at high-level $(18:2)_3$-MLCL addition. The within-day coefficients of variation (CVs) at low and high levels of addition were 12.3% and 2.8%, respectively. The between-day CVs at low and high levels of addition were 17.3% and 4.2%, respectively. We used this validated method to determine the levels of both CLs and MLCLs in lymphoblasts, lymphocytes, fibroblasts, muscle, and heart of controls and BTHS patients.

MLCL and CL analysis in BTHS cells

Figure 1 shows the MLCL molecular species isolated from cultured lymphoblasts of a control and a BTHS patient. The spectra in Fig. 1 are representative of those observed in three control and three BTHS lymphoblast cell lines. This figure clearly shows that the levels of $(18:1)_3$-MLCL (*m/z* 595.5), $(16:0)/(18:1)_2$-MLCL (*m/z* 582.5), $(16:1)/(18:1)_2$-MLCL (*m/z* 581.5), and $(16:0)_2/(18:1)$-MLCL (*m/z* 568.5) are highly increased in BTHS lymphoblasts (Fig. 1A) compared with control cells (Fig. 1B). Semiquantitative analysis showed that the levels of MLCL species in BTHS were 5–20 times higher than in controls (Fig. 1C). **Figure 2** shows the CL molecular species in the same lymphoblast samples. Five clusters of doubly charged ions corresponding to different CL molecular species are present in the control sample (Fig. 2A). The degree of saturation of the fatty acyl side chains increases with higher *m/z* values within such a cluster. The mass difference between each cluster corresponds to CLs with fatty acyl side chains of different lengths. For example, 727.5 corresponds to a $(18:1)_4$-CL, whereas 713.5 corresponds to $(16:1)/(18:1)_3$-CL. In Fig. 2A, B, the CL clusters are numbered 1, 2, 3, 4, and 5. In controls, the most abundant CL molecular species are present in clusters 3 and 4, which contain 18:2, 18:1, and 16:1 as fatty acyl side chains. Cluster 5 also contains unsaturated C_{20} fatty acids in addition to 18:2 and 18:1. Compared with the CL molecular species in control cells (Fig. 2A), the most unsaturated CLs in all clusters (e.g., the peaks with the lowest *m/z* of the cluster) are decreased significantly in BTHS cells (Fig. 2B), whereas the levels of less unsaturated CLs in each cluster, such as $(18:1)_4$-CL (*m/z* 727.5), are present in normal amounts (Fig. 2C).

Because of the presence of MLCLs in BTHS lymphoblasts, we investigated the MLCL/CL profile of BTHS (n = 5) and control (n = 9) lymphocytes to determine whether these untransformed BTHS cells also display an accumulation of these aberrant CL species. Surprisingly, the CL spectra of control lymphoblasts and lymphocytes were very dissimilar. We found that $(18:2)_4$-CL is the most abundant CL in control lymphocytes (**Fig. 3A**), whereas lymphoblasts contain more saturated CL species and display a larger variety of acyl side chain length (compare Figs. 2A and 3A). As in BTHS lymphoblasts, we did observe a severe CL deficiency and a clear accumulation of MLCLs in BTHS lymphocytes (Fig. 3B, C). This is in contrast to BTHS platelets (n = 8) and fibroblasts (n = 6), in which MLCL accumulation was very marginal or even absent (data not shown).

MLCL and CL analysis in BTHS tissues

Because heart and muscle contain high amounts of CL and BTHS patients present with symptoms related to these tissues [(cardio)myopathy], we investigated the CLs and MLCLs in these tissues of two control subjects and two BTHS patients. In control heart, $(18:2)_4$-CL (*m/z* 723.5) is the most abundant CL (**Fig. 4A, C**, left graph). This CL is severely deficient in BTHS heart, whereas other CLs, including $(18:1)/(18:2)_3$-CL (*m/z* 724.5), $(18:1)_2/(18:2)_2$-CL (*m/z* 725.5), $(18:1)_3/(18:2)_1$-CL (*m/z* 726.5), and $(18:1)_4$-CL (*m/z* 727.6), are still present and their levels even appear to be slightly increased compared with control heart (Fig. 4B, C, right graph). The CL spectrum of skeletal muscle in both control (n = 2) and BTHS (n = 2) was very similar to that of heart (data not shown).

In control heart (**Fig. 5A**) as well as muscle (data not shown), we detected one MLCL species with the fatty acid composition $(18:2)_3$-MLCL (*m/z* 592.5), which is present in low amounts compared with $(18:2)_4$-CL. In BTHS heart and muscle, however, there is a clear accumulation of different MLCLs, namely $(18:1)_3$-MLCL (*m/z* 595.5), $(18:1)_2/(18:2)$-MLCL (*m/z* 594.5), $(16:0)/(18:1)_2$-MLCL (*m/z* 582.5), and $(16:1)/(18:1)_2$-MLCL (*m/z* 581.5) (Fig. 5B). None of these MLCL molecular species were detectable in control samples. The levels of these MLCL molecular species were 10 times higher in BTHS than in control samples (Fig. 5C) and were present in similar quantities as the remaining CLs. The levels of $(18:2)_3$-MLCL in BTHS seemed to remain in the same range as in controls (Fig. 5C).

Analysis of other phospholipids

Using the same HPLC-tandem MS system, we investigated the composition and abundance of other phospholipids, including PE and PC, in the same BTHS and control tissues used for the (ML)CL analysis. **Figure 6** shows clear abnormalities in PE molecular species isolated from heart tissue of a control (Fig. 6A) and a BTHS (Fig. 6B) heart sample. 18:0/18:2-PE level (*m/z* 744.8) was five to six times higher in BTHS heart compared with control heart (Fig. 6B). The fatty acid composition of this PE, 18:0/18:2, was confirmed by tandem MS. The same abnormalities were found in the PC fraction but were less prominent compared with PE. 34:2-PC levels (*m/z* 758.8) (**Fig. 7**) appeared to be at least two to three times higher in BTHS samples compared with controls. This PC likely corresponds to 16:0/18:2 fatty acid composition, although this

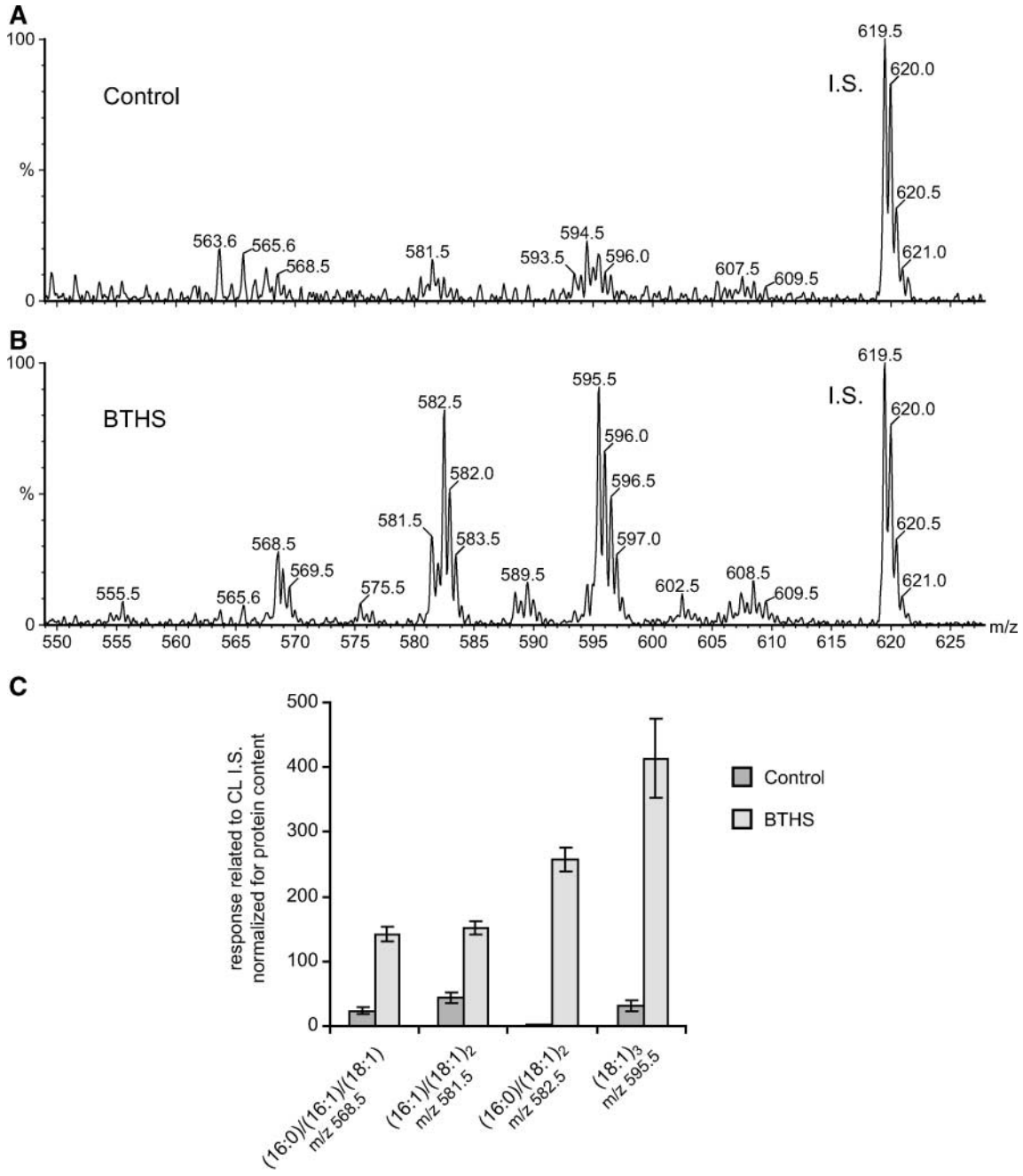

Fig. 1. Representative mass spectra of monolysocardiolipin (MLCL) molecular species in control and Barth syndrome (BTHS) lymphoblasts. The same amount of cellular protein (2 mg) was extracted for both control and BTHS samples. The peak at *m/z* 619.5 corresponds to the $(14:0)_4$-cardiolipin (CL), the internal standard (I.S.). In both control (A) and BTHS (B) lymphoblasts, three different MLCL clusters are present; however, MLCL levels are highly increased in BTHS lymphoblasts. A semiquantitative representation of the levels of selected MLCLs, including their fatty acid composition, is depicted in C. These values are averages ± SD from three different control and BTHS lymphoblast cell lines.

was not checked experimentally. Additionally, *m/z* 742.9 in Fig. 6D, which likely represents a 16:0-enyl/C18:2 acyl-PC (a plasmalogen), appears to be increased in BTHS heart. Both PE and PC molecular species containing arachidonic acid (*m/z* values indicated by arrows in Fig. 6B, D) seemed to be decreased in BTHS samples. We did not observe abnormalities in other investigated phospholipid classes, including phosphatidylglycerol, phosphatidylinositol, and phosphatidylserine.

MLCL and CL deficiency and apoptosis

Recently, it was shown that CL and MLCL bind to Bid, a proapoptotic Bcl-2 family member, which is involved in death receptor-mediated apoptosis in many cell systems (23, 24). Upon an apoptotic stimulus, cytosolic Bid is somehow recruited to the mitochondrial membrane, where, in concert with other Bcl-2 family members, it initiates the release of apoptogenic factors such as cytochrome *c*, thereby promoting apoptosome-mediated apoptosis. In this pro-

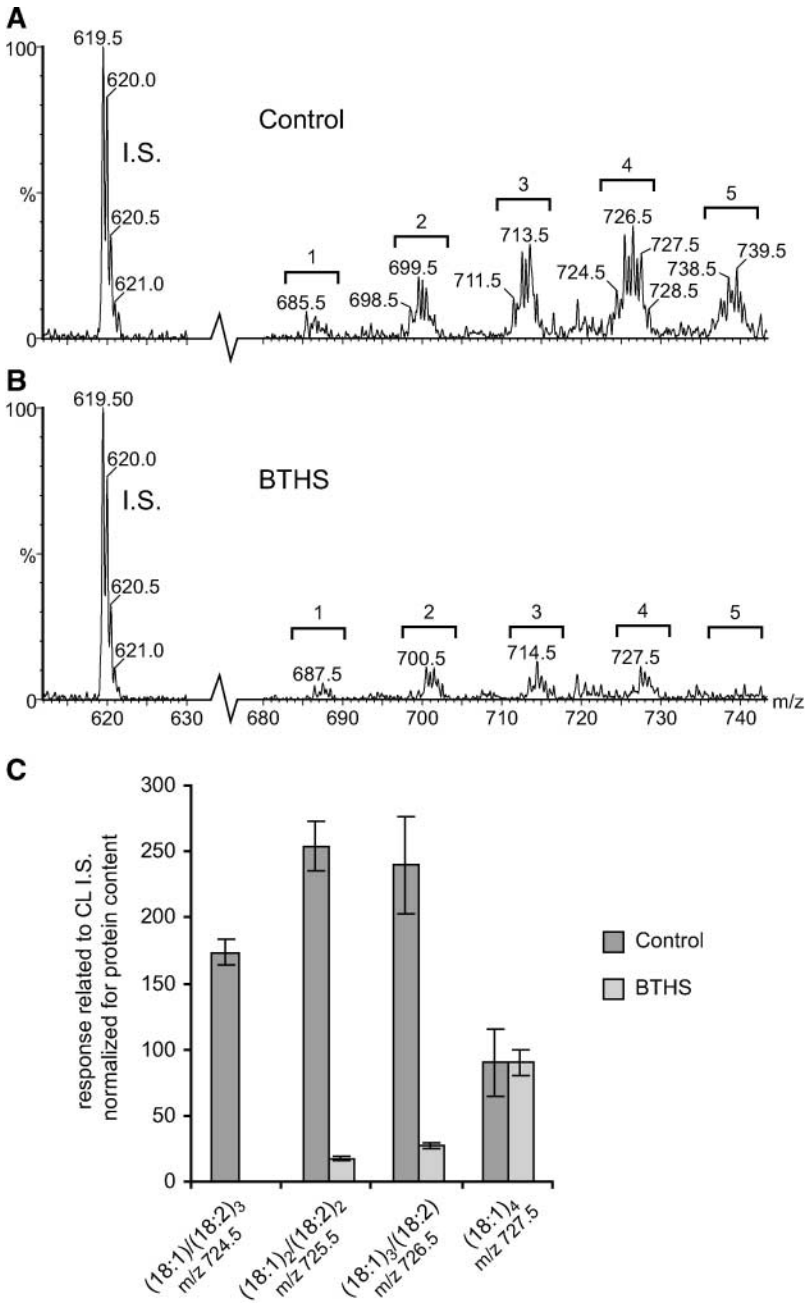

Fig. 2. Representative mass spectra of CL molecular species in cultured control and BTHS lymphoblasts (same samples used in Fig. 1). The same amount of cellular protein (2 mg) was extracted for both control and BTHS samples. The peak at *m/z* 619.5 corresponds to the $(14:0)_4$-CL, the I.S. A: In control lymphoblasts, five different CL clusters are present. B: BTHS lymphoblasts clearly display CL deficiency, especially those with a high degree of unsaturation [e.g., the peaks within a CL cluster with low *m/z* (*m/z* 698.5, 711.5, and 724.5)]. A semiquantitative representation of the levels of selected CLs, including their fatty acid composition, is depicted in C. These values are averages ± SD from three different control and BTHS lymphoblast cell lines.

cess, full-length Bid is cleaved by caspase-8, resulting in a truncated protein termed tBid, which is considered the active form. Esposti and coworkers (24) have shown that although both CL and MLCL interact in vitro with (t)Bid, MLCL binds with higher affinity and also is capable of stimulating the cytochrome *c*-releasing capacity of tBid. The observation that, in vivo, MLCL levels increase upon Fas-induced apoptosis suggests that MLCL production in mitochondria could be involved in the initiation of apoptosis by the recruitment of (t)Bid to mitochondria. Therefore, we hypothesized that the accumulation of MLCLs in BTHS cells and tissues could result in enhanced apoptosis, which may play a role in the pathogenesis in BTHS. To test this hypothesis, we used BTHS lymphoblasts, which were found to accumulate MLCLs, and studied several relevant apoptotic parameters.

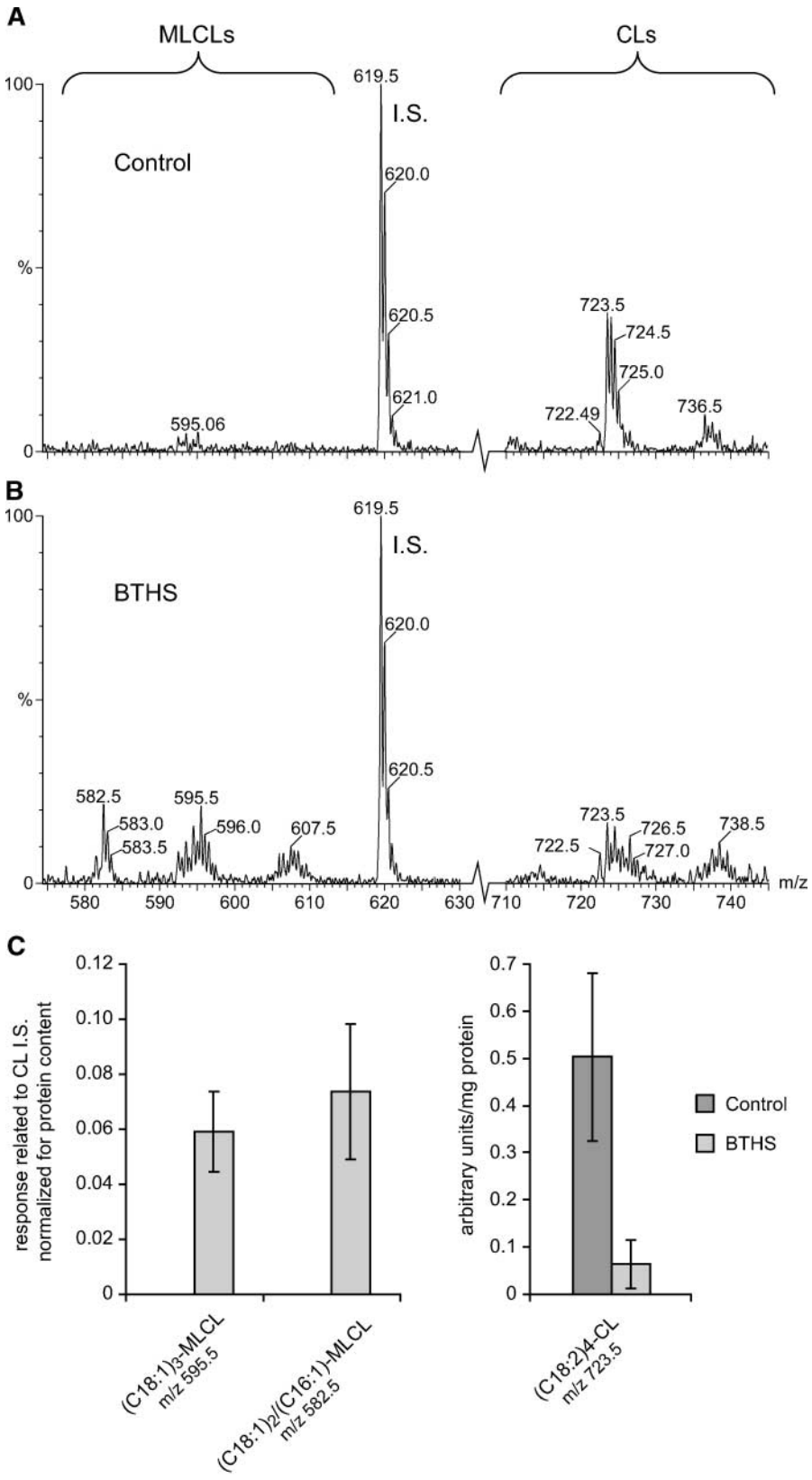

Fig. 3. Mass spectra of CL and MLCL molecular species from control and BTHS lymphocytes. The peak at *m/z* 619.5 corresponds to the $(14:0)_4$-CL, the I.S. $(18:2)_4$-CL (*m/z* 723.5), which is the most abundant CL in control lymphocytes (A), is decreased markedly in BTHS lymphocytes (B). As in lymphoblasts, three different clusters representing MLCLs are present in BTHS lymphocytes that are (virtually) not detectable in control lymphocytes. A semiquantitative representation of the levels of selected MLCLs (left graph) and CLs (right graph), including their fatty acid composition, is depicted in C. These values are averages ± SD from different control (n = 9) and BTHS (n = 5) lymphocytes.

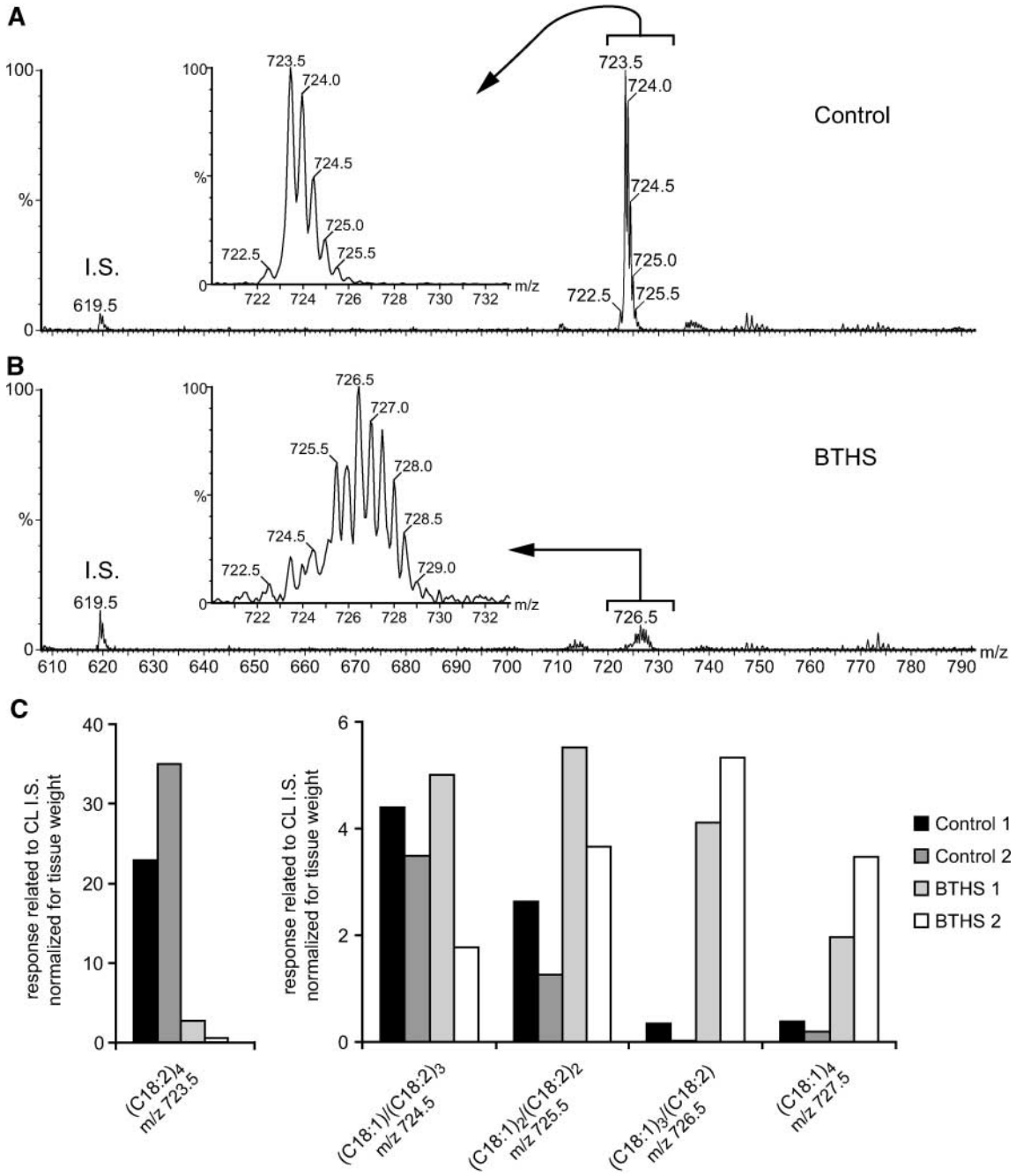

Fig. 4. Mass spectra of CL molecular species from control and BTHS heart tissue. The peak at *m/z* 619.5 corresponds to the $(14:0)_4$-CL, the I.S. A: As in lymphocytes, $(18:2)_4$-CL is the most abundant CL found in heart tissue of the control sample. B: The levels of this CL are dramatically decreased in the BTHS heart. A semiquantitative representation of the levels of selected CLs in two control and two BTHS hearts, including their fatty acid composition, is depicted in C. This clearly shows that although there is a profound deficiency of $(18:2)_4$-CL (left graph), the less unsaturated CL molecular species are present at normal or even higher levels in BTHS heart (right graph).

First, we investigated several apoptotic markers in unstimulated cells. After induction of apoptosis, PARP is cleaved by caspase-3, which prevents PARP from repairing apoptosis-induced DNA damage. Figure 7A shows that, as in control cells, there is no cleavage of PARP in BTHS lymphoblasts and that most, if not all, of the protein is full length. Second, we determined the subcellular distribution of (t)Bid and cytochrome *c* in three BTHS and three control lymphoblast cell lines. Figure 7B, C show that there is no difference between the distribution of Bid and cytochrome *c* in mitochondria and cytosol in BTHS and control lymphoblasts. Bid is present as full-length Bid and detected only in the cytosol. In contrast, cytochrome *c* is found only in mitochondria and is not present in the cytosol. The distribution of the mitochondrial enzyme glutamate dehydrogenase confirms that the mitochondria were intact and well separated from the cytosol (Fig. 7C).

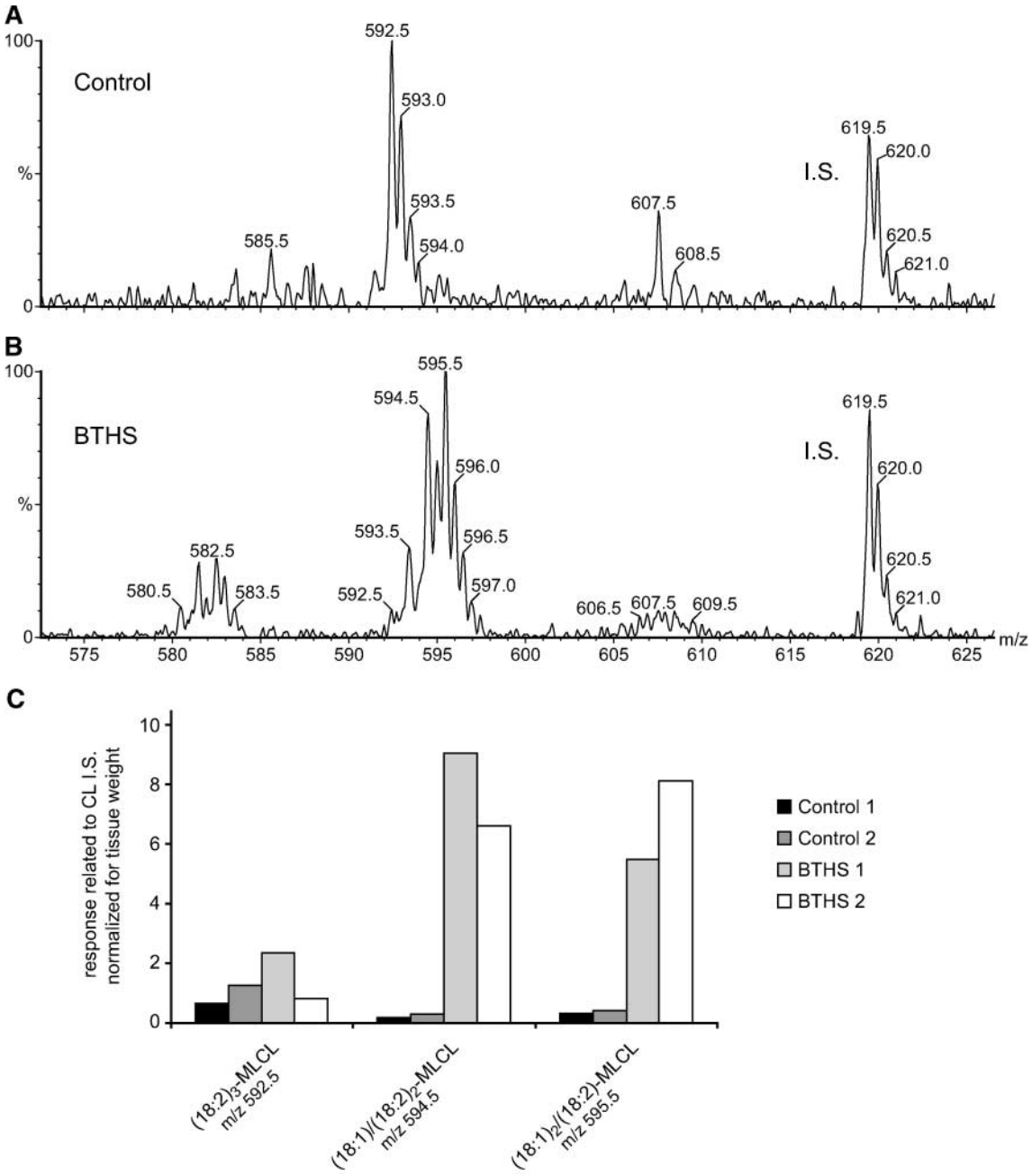

Fig. 5. Mass spectra of MLCL molecular species from control and BTHS heart tissue. The peak at *m/z* 619.5 corresponds to the $(14:0)_4$-CL, the I.S. In control heart (A), only $(18:2)_3$-MLCL (*m/z* 592.5) was observed, whereas in BTHS heart (B), there was a clear accumulation of more saturated MLCLs. A semiquantitative representation of the levels of selected MLCLs in two control and two BTHS hearts, including their fatty acid composition, is depicted in C.

Next, we investigated whether BTHS cell lines showed any differences in susceptibility to death receptor-mediated apoptosis. Lymphoblasts from three BTHS patients and three controls were incubated for 24 h with increasing concentrations of supernatant containing membrane-bound FasL. A Jurkat, human T-lymphoma cell line was used as a positive control, as these cells express substantial levels of Fas receptor (25). As expected, Jurkat cells showed a high degree of cell death (~80%) even at high dilution (1:10) of FasL (**Fig. 8A**). Lymphoblasts from three controls and three BTHS patients were also susceptible to FasL-induced cell death. Higher FasL levels were required to elicit cell death than for Jurkat cells, with maximal cell death of ~50% at 2:3 FasL dilution. BTHS and control cell lines showed no apparent differences in FasL sensitivity (Fig. 8A).

Binding of membrane-bound FasL to the Fas receptor is expected to result in the cleavage and activation of caspase-8, which in turn cleaves Bid, allowing tBid to translocate to the mitochondria. In keeping with the results of FasL sensitivity, the kinetics of caspase-8 activation and Bid cleavage were somewhat slower in control and BTHS lym-

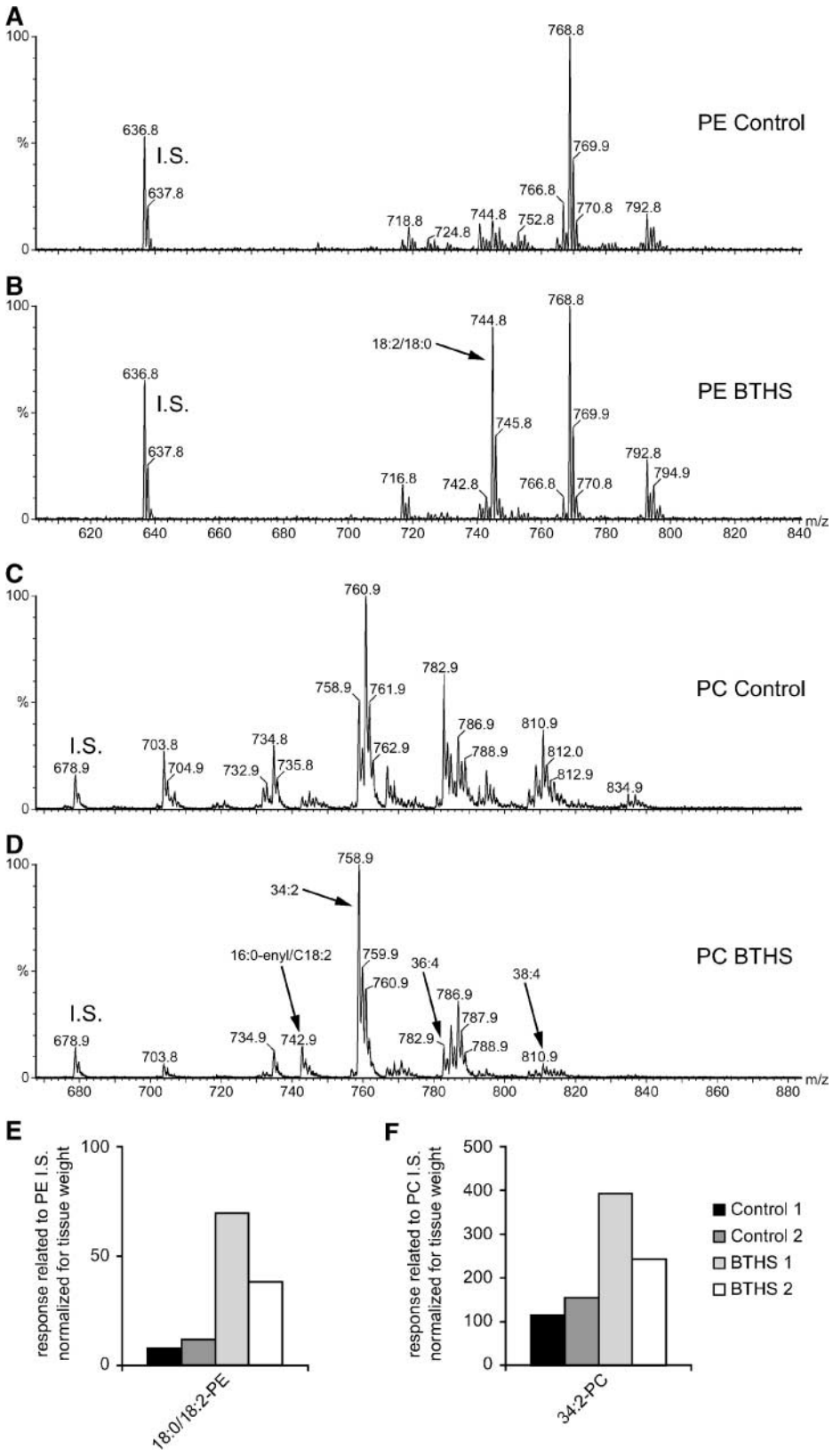

Fig. 6. Mass spectra of phosphatidylethanolamine (PE) and phosphatidylcholine (PC) molecular species in control and BTHS heart. PE molecular species found in control (A) and BTHS (B) are shown. The peak at *m/z* 636.8 in both PE spectra corresponds to the $(14:0)_2$-PE, which was used as I.S. 18:0/18:2-PE (*m/z* 744.8) clearly accumulates in both BTHS hearts (B, E). Compared with the control (C), the level of 34:2-PC (*m/z* 758.9, probably 16:0/18:2-PC) in BTHS (D, F) was increased. In addition, the levels of arachidonic acid containing PE and PC (36:4 and 38:4) seemed to be decreased in BTHS (*m/z* values are indicated by arrows in B, D). 16:0-enyl/18:2-acyl-PC (*m/z* 742.9), a plasmalogen, appears to be increased in BTHS. Semiquantitative representations of the levels of 18:0/18:2-PE and 36:2-PC in two control and two BTHS hearts are depicted in E, F, respectively.

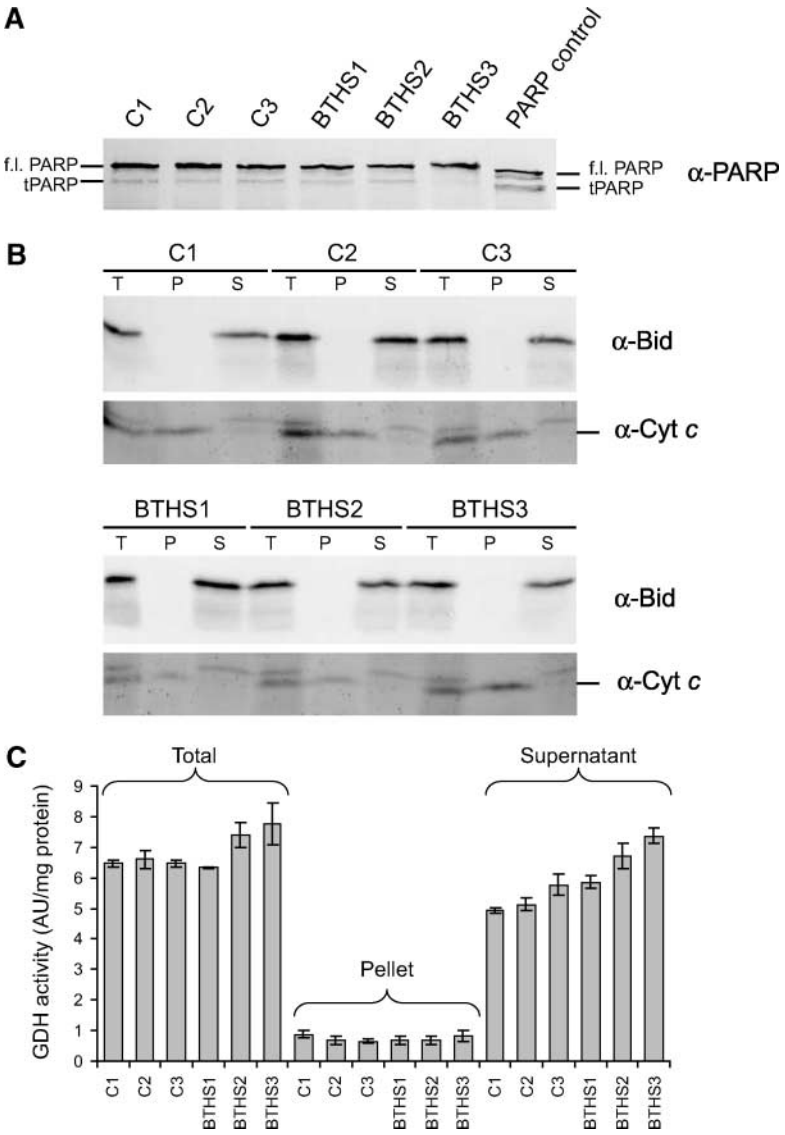

Fig. 7. Analysis of apoptotic parameters in control and BTHS lymphoblasts. A: Poly (ADP-ribose) polymerase (α-PARP) immunoblot analysis of three control (C1–C3) and three BTHS (BTHS1–BTHS3) lymphoblasts and a PARP control containing both full-length (f.l. PARP) and truncated (tPARP) PARP. There is no cleavage of PARP in BTHS lymphoblasts, and most, if not all, of the protein is full length. B: Subcellular distribution of BH3-interacting domain death agonist (Bid) and cytochrome *c* in control and BTHS lymphoblasts analyzed by immunoblot analysis using anti-Bid and anti-cytochrome *c* (α-Bid and α-Cyt c) antibodies. P, pellet; S, supernatant; T, total. There is no difference between the distribution of Bid and cytochrome *c* between mitochondria and cytosol in BTHS and control lymphoblasts. C: The integrity of the mitochondria is confirmed by the distribution of the mitochondrial enzyme glutamate dehydrogenase (GDH) between the organelle and cytosolic fractions. GDH activity was measured in triplicate. Error bars represent standard deviation of the three measured activities. AU, arbitrary units.

phoblasts than in Jurkat cells (Fig. 8B). Whole cell lysates of BTHS and control lymphoblasts showed comparable rates of caspase-8 activation, as indicated by the loss of the higher molecular mass species and the appearance of the activated 43/41 kDa and smaller 18 kDa subunits. Immunoblotting showed comparable rates of Bid cleavage in cytosolic fractions from FasL-treated BTHS and control cells, as indicated by the disappearance of the 22 kDa band (Fig. 8C). However, we were unable to detect accumulation of tBid reliably in membrane (data not shown) or cytosolic fractions or in whole cell lysate from any cell types. Because we could not make a direct comparison of the kinetics of tBid translocation to the membrane fraction in control and BTHS cells, we studied the binding of tBid to isolated mitochondria. Mitochondria from control and BTHS cells were incubated with 1 μg/ml recombinant tBid for 1 h at 30°C, and mitochondrial pellets were analyzed by immunoblotting with anti-Bid antibody. There was no apparent difference in the amount of tBid bound to control and BTHS mitochondria (data not shown).

DISCUSSION

Based on the recent finding that the yeast disruptant of the *TAZ* ortholog in *Saccharomyces cerevisiae* not only displays CL deficiency but also accumulates MLCLs (18, 19), we set out to investigate whether MLCL accumulation also occurs in BTHS. Therefore, we successfully adapted our method to enable the measurement of MLCLs in addition to CL and other phospholipids. As observed in the yeast model for BTHS, our data show an accumulation of MLCL molecular species in some BTHS cell lines and tissues. We found that MLCLs accumulate in BTHS heart, muscle, (cultured Epstein-Barr virus-transformed) lymphoblasts, and lymphocytes. In contrast, virtually no MLCL accumulation was observed in cultured primary fibroblasts and platelets of BTHS patients. The accumulation of a supposed intermediate of CL remodeling in BTHS further supports the earlier suggestion that the decreased levels of CL in BTHS are attributable to a defect in the remodeling process. Given that the BTHS phenotype shows considerable variability, even in individuals carrying the same mu-

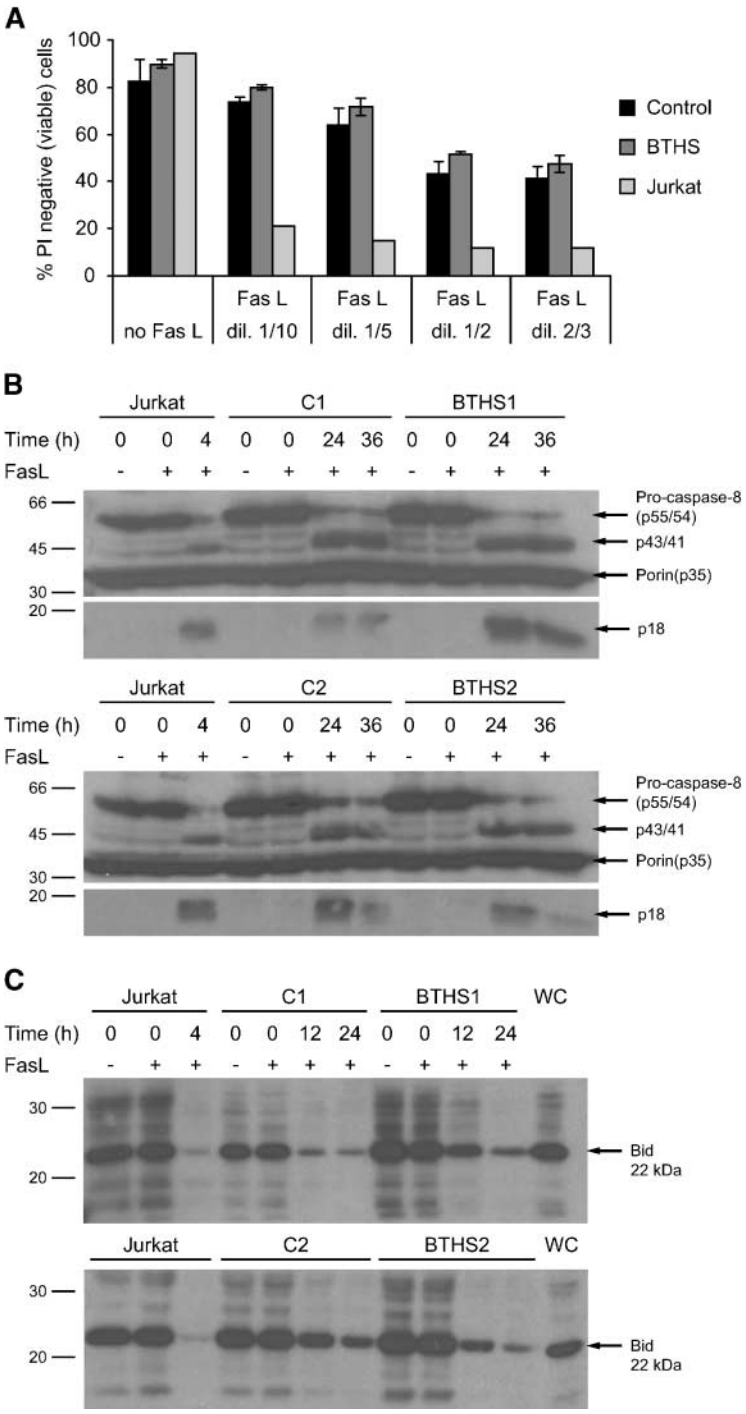

Fig. 8. Receptor-mediated death in Epstein-Barr virus-transformed B-lymphoblasts incubated with membrane-bound Fas ligand (FasL). A: Jurkat cells and control and BTHS lymphoblast cell lines were treated for 24 h with decreasing dilutions of FasL supernatant, and viability was determined by staining with 1 μg/ml propidium iodide (PI) and flow cytometry. Error bars represent SD for three different control and three different BTHS patient cell lines. B: Immunoblot of caspase-8 activation for two control and two BTHS patient lymphoblast cell lines. At 0 h, each cell line was suspended in undiluted culture supernatant with membrane-bound FasL (+) or in undiluted supernatant with no FasL (−). Cells were incubated for the indicated times, and whole cell lysates were analyzed by immunoblot analysis using anti-caspase-8 antibody with anti-porin as a loading control. The two isomeric products at 55 and 54 kDa represent the procaspase-8 form and the 43/41 kDa (isomers), and the 18 kDa bands are the active products. C: Immunoblots of BH3-interacting domain death agonist (Bid) cleavage in cytosolic fractions of two control and two BTHS cell lines treated with FasL as described above. Cells were incubated for the indicated times, and cytosolic fractions were analyzed by immunoblot analysis using anti-Bid antibody. Each blot also includes a whole cell lysate (WC) sample from an untreated cell line as a marker of full-length Bid at 22 kDa.

tation, it is an interesting possibility that the amount of MLCL accumulation in different tissues/cells might correlate with the individual patient phenotype. Studies to investigate this are currently under way.

The fact that some cell types show high accumulation of MLCLs and others show virtually no accumulation of these metabolites is surprising and suggests that remodeling of CLs may be different in different cell types or tissues. It has been known for some time that CL is remodeled via the deacylation/reacylation mechanism (17), with MLCL as an obligate intermediate. The enzyme responsible for the acyl-CoA-dependent reacylation of MLCL, MLCL acyltransferase, has been purified from pig liver mitochondria by Taylor and Hatch (16), but the corresponding gene has not been identified. Recently, a murine gene termed ALCAT1 has been identified that encodes an acyl-CoA:lysocardiolipin acyltransferase (26). This enzyme recognizes both MLCL and dilysocardiolipin as substrates, with a preference for linoleoyl-CoA and oleoyl-CoA as acyl donors. Remarkably, this enzyme appears to be localized in the endoplasmic reticulum, as opposed to the mitochondrial localization reported by Taylor and Hatch (16). Whether ALCAT1 indeed encodes the enzyme purified by those authors, or

more than one acyltransferase exists that can reacylate MLCLs, remains to be established.

Recently, Xu et al. (27) reported that in rat liver, both CL and MLCL can also be remodeled via transacylation, using PC and PE as acyl donors. They showed that the acyl transfer activity in rat liver mitochondria was specific for linoleate-containing phospholipids, in contrast to lymphoblasts, in which PE containing oleate could also be used as an acyl donor. The mere fact that MLCLs accumulate in certain tissues, however, does not allow discrimination between the involvement of deacylation/reacylation and transacylation mechanisms, because MLCL formation theoretically occurs in both processes. Still, analysis of the fatty acid composition of the accumulating MLCL molecular species could contribute to our understanding of the CL remodeling process. When considering this, there appears to be a direct relation between the fatty acid composition of the MLCLs and that of the CLs of a certain tissue or cell type. In control heart and muscle samples, we only found one MLCL molecular species, $(18:2)_3$-MLCL, the lysoderivative of $(18:2)_4$-CL. In general, MLCL molecular species in BTHS tissues and cells were predominantly composed of monounsaturated and saturated fatty acids, which also reflected the composition of the remaining CLs. This was also true for the accumulating MLCLs in lymphoblasts and lymphocytes, which again reflect the CL fatty acid composition. Xu et al. (27) observed that the transacylase activity for oleate-containing PE was reduced in lymphoblasts from patients with BTHS, which led them to suggest that CL is remodeled by acyl-specific phospholipid transacylation, which involves tafazzin. If this is true, MLCL acyltransferase is encoded by a different gene, which is supported by the recent identification of ALCAT1. The observation that not all cell types display MLCL accumulation could reflect the expression pattern of ALCAT1 (or that of an enzyme with similar activity). This could imply that tissues with low or no expression of MLCL acyltransferase are less capable or incapable of reacylating MLCLs, which then accumulate. Obviously, another factor could be the activities of the different phospholipases, which are needed for the generation of MLCLs. Because the fatty acid composition of the MLCLs parallels that of the CLs, it is likely that the formation of MLCLs is not a specific process. This in turn is in agreement with the observed substrate specificity of the MLCL acyltransferase isolated by Taylor and Hatch (16), which is capable of using linoleoyl-, oleoyl-, and even palmitoyl-CoA, albeit less efficiently. This less specific reacylation of MLCL could be followed by a more linoleoyl-specific transacylation reaction involving tafazzin, resulting in the formation of the predominant tetralinoleoylcardiolipin. The existence of such a mechanism is supported by the fact that PC and PE molecular species containing linoleic acid, which are reported to function as acyl donors in the transacylation of CL, accumulate in BTHS (27, this study). The results of Xu et al. (27) demonstrated that the transacylation reaction has a high specificity for linoleoyl-containing PC or PE in rat liver. In fact, palmitoyl- and oleoyl-containing PC or PE were totally ineffective donors in the transacylation reaction. It is noteworthy, however, that although in liver the transacylation reaction was very specific for linoleoyl-containing donors, in lymphoblasts this transacylation could also be performed with oleoyl-containing PE (27). This suggests that there may be a tissue-dependent substrate specificity for the transacylation reaction or that multiple enzymes exist with different substrate specificities.

Interestingly, both the CL synthase yeast deletion mutant *crd1*Δ (28–30) and the yeast tafazzin disruptant *taz1*Δ (18) both show increased total PE levels, especially when grown on nonfermentable carbon sources. Like CL, PE is a non-bilayer-forming phospholipid. The nonbilayer structure is formed preferably in membrane regions with a high curvature of the lipid bilayer, such as the cristae of the inner mitochondrial membrane (31). In parallel to what was proposed for *crd1*Δ (30), an alternative explanation for the accumulation of linoleyl-containing PE species in BTHS heart could also be that these linoleyl-containing PEs compensate for the decreased mitochondrial CL levels and abnormal CL composition.

Because MLCLs recently were suggested to promote apoptosis by binding the proapoptotic protein tBid and its concomitant recruitment to the mitochondrial outer membrane (24), we investigated whether BTHS lymphoblasts displayed a higher level of basal or stimulated apoptosis. Cleavage of PARP and the subcellular distribution of (t)Bid and cytochrome *c* were comparable in BTHS and control cells. Control and BTHS lymphoblasts also showed similar kinetics of cell death induced by membrane-bound FasL and similar kinetics of caspase-8 activation and Bid cleavage. We were unable to directly assess the kinetics of tBid translocation to mitochondria in intact cells from BTHS patients and controls, because we could not detect significant accumulation of tBid in membrane fractions, despite the pronounced Bid cleavage. This is most likely the result of the rapid turnover of tBid, which has been reported to occur in other cell types by ubiquitination and proteasomal degradation, with a half-life of ~1.5 h (32). Isolated mitochondria prepared from BTHS and control lymphoblasts showed no apparent differences in tBid binding. Thus, these studies imply that BTHS and control lymphoblasts show comparable rates of Bid-mediated apoptotic cell death. Although these results are in agreement with the findings of Kuijpers and coworkers (33), who showed that BTHS neutrophils are not apoptotic even though they are annexin-V-positive, MLCL could still have different effects in other cell types. Also, one should keep in mind that the lymphoblasts used for these studies are Epstein-Barr virus-transformed cells; further investigations in freshly isolated BTHS blood cells are currently under way.

The observation that MLCLs accumulate in lymphocytes also has an impact on the way BTHS is diagnosed. Previously, we published a method to diagnose BTHS patients by analyzing CL levels in platelets using HPLC-MS (8). Although this method has been and still is very useful, it is based on a decrease of CL levels, which has less diagnostic power than the accumulation of (what appears to

be) a disease-specific compound. We are now investigating whether the determination of both MLCL and CL levels (and possibly a ratio of these two) in lymphocytes is a better diagnostic parameter for BTHS.

This work was supported by a grant from the Prinses Beatrix Fund (The Hague, The Netherlands; Grant MAR01-0129 to R.J.A.W.), the Barth Syndrome Foundation (grant to F.M.V.), the National Health and Medical Research Council of Australia (grant to D.R.T.), and the National Institutes of Health, National Heart, Lung, and Blood Institute (Grant P01 HL-67155 to J.A.T). The authors thank Dr. M. Schlame for arranging the BTHS heart tissues, Dr. T. W. Kuijpers and N. A. Maianski for the Bid and cytochrome *c* antibodies, and Dr. C. Hawkins for the Neuro2A-CD95L and Neuro2A-neo cell lines.

REFERENCES

1. Barth, P. G., H. R. Scholte, J. A. Berden, J. M. Van der Klei-Van Moorsel, I. E. Luyt-Houwen, E. T. Van't Veer-Korthof, J. J. Van der Harten, and M. A. Sobotka-Plojhar. 1983. An X-linked mitochondrial disease affecting cardiac muscle, skeletal muscle and neutrophil leucocytes. *J. Neurol. Sci.* **62:** 327–355.
2. Kelley, R. I., J. P. Cheatham, B. J. Clark, M. A. Nigro, B. R. Powell, G. W. Sherwood, J. T. Sladky, and W. P. Swisher. 1991. X-linked dilated cardiomyopathy with neutropenia, growth retardation, and 3-methylglutaconic aciduria. *J. Pediatr.* **119:** 738–747.
3. Barth, P. G., F. Valianpour, V. M. Bowen, J. Lam, M. Duran, F. M. Vaz, and R. J. Wanders. 2004. X-linked cardioskeletal myopathy and neutropenia (Barth syndrome): an update. *Am. J. Med. Genet.* **126A:** 349–354.
4. Barth, P. G., R. J. Wanders, P. Vreken, E. A. Janssen, J. Lam, and F. Baas. 1999. X-linked cardioskeletal myopathy and neutropenia (Barth syndrome) (MIM 302060). *J. Inherit. Metab. Dis.* **22:** 555–567.
5. Bione, S., P. D'Adamo, E. Maestrini, A. K. Gedeon, P. A. Bolhuis, and D. Toniolo. 1996. A novel X-linked gene, G4.5, is responsible for Barth syndrome. *Nat. Genet.* **12:** 385–389.
6. Neuwald, A. F. 1997. Barth syndrome may be due to an acyltransferase deficiency. *Curr. Biol.* **7:** R465–R466.
7. Vreken, P., F. Valianpour, L. G. Nijtmans, L. A. Grivell, B. Plecko, R. J. Wanders, and P. G. Barth. 2000. Defective remodeling of cardiolipin and phosphatidylglycerol in Barth syndrome. *Biochem. Biophys. Res. Commun.* **279:** 378–382.
8. Valianpour, F., R. J. Wanders, P. G. Barth, H. Overmars, and A. H. van Gennip. 2002. Quantitative and compositional study of cardiolipin in platelets by electrospray ionization mass spectrometry: application for the identification of Barth syndrome patients. *Clin. Chem.* **48:** 1390–1397.
9. Valianpour, F., R. J. Wanders, H. Overmars, P. Vreken, A. H. Van Gennip, F. Baas, B. Plecko, R. Santer, K. Becker, and P. G. Barth. 2002. Cardiolipin deficiency in X-linked cardioskeletal myopathy and neutropenia (Barth syndrome, MIM 302060): a study in cultured skin fibroblasts. *J. Pediatr.* **141:** 729–733.
10. Schlame, M., J. A. Towbin, P. M. Heerdt, R. Jehle, S. DiMauro, and T. J. Blanck. 2002. Deficiency of tetralinoleoyl-cardiolipin in Barth syndrome. *Ann. Neurol.* **51:** 634–637.
11. Schlame, M., R. I. Kelley, A. Feigenbaum, J. A. Towbin, P. M. Heerdt, T. Schieble, R. J. Wanders, S. DiMauro, and T. J. Blanck. 2003. Phospholipid abnormalities in children with Barth syndrome. *J. Am. Coll. Cardiol.* **42:** 1994–1999.
12. Schlame, M., D. Rua, and M. L. Greenberg. 2000. The biosynthesis and functional role of cardiolipin. *Prog. Lipid Res.* **39:** 257–288.
13. Hatch, G. M. 1998. Cardiolipin: biosynthesis, remodeling and trafficking in the heart and mammalian cells [review]. *Int. J. Mol. Med.* **1:** 33–41.
14. Schlame, M., S. Brody, and K. Y. Hostetler. 1993. Mitochondrial cardiolipin in diverse eukaryotes. Comparison of biosynthetic reactions and molecular acyl species. *Eur. J. Biochem.* **212:** 727–735.
15. Schlame, M., K. Beyer, M. Hayer-Hartl, and M. Klingenberg. 1991. Molecular species of cardiolipin in relation to other mitochondrial phospholipids. Is there an acyl specificity of the interaction between cardiolipin and the ADP/ATP carrier? *Eur. J. Biochem.* **199:** 459–466.
16. Taylor, W. A., and G. M. Hatch. 2003. Purification and characterization of monolysocardiolipin acyltransferase from pig liver mitochondria. *J. Biol. Chem.* **278:** 12716–12721.
17. Schlame, M., and B. Rustow. 1990. Lysocardiolipin formation and reacylation in isolated rat liver mitochondria. *Biochem. J.* **272:** 589–595.
18. Gu, Z., F. Valianpour, S. Chen, F. M. Vaz, G. A. Hakkaart, R. J. Wanders, and M. L. Greenberg. 2004. Aberrant cardiolipin metabolism in the yeast taz1 mutant: a model for Barth syndrome. *Mol. Microbiol.* **51:** 149–158.
19. Vaz, F. M., R. H. Houtkooper, F. Valianpour, P. G. Barth, and R. J. Wanders. 2003. Only one splice variant of the human TAZ gene encodes a functional protein with a role in cardiolipin metabolism. *J. Biol. Chem.* **278:** 43089–43094.
20. Vaz, F. M., R. Ofman, K. Westinga, J. W. Back, and R. J. Wanders. 2001. Molecular and biochemical characterization of rat epsilon-n-trimethyllysine hydroxylase, the first enzyme of carnitine biosynthesis. *J. Biol. Chem.* **276:** 33512–33517.
21. Knight, M. J., C. D. Riffkin, P. G. Ekert, D. M. Ashley, and C. J. Hawkins. 2004. Caspase-8 levels affect necessity for mitochondrial amplification in death ligand-induced glioma cell apoptosis. *Mol. Carcinog.* **39:** 173–182.
22. Silke, J., T. Kratina, P. G. Ekert, M. Pakusch, and D. L. Vaux. 2004. Unlike Diablo/smac, Grim promotes global ubiquitination and specific degradation of X chromosome-linked inhibitor of apoptosis (XIAP) and neither cause apoptosis. *J. Biol. Chem.* **279:** 4313–4321.
23. Esposti, M. D. 2004. Mitochondria in apoptosis: past, present and future. *Biochem. Soc. Trans.* **32:** 493–495.
24. Esposti, M. D., I. M. Cristea, S. J. Gaskell, Y. Nakao, and C. Dive. 2003. Proapoptotic Bid binds to monolysocardiolipin, a new molecular connection between mitochondrial membranes and cell death. *Cell Death Differ.* **10:** 1300–1309.
25. Strasser, A., A. W. Harris, D. C. Huang, P. H. Krammer, and S. Cory. 1995. Bcl-2 and Fas/APO-1 regulate distinct pathways to lymphocyte apoptosis. *EMBO J.* **14:** 6136–6147.
26. Cao, J., Y. Liu, J. Lockwood, P. Burn, and Y. Shi. 2004. A novel cardiolipin-remodeling pathway revealed by a gene encoding an endoplasmic reticulum-associated acyl-CoA:lysocardiolipin acyltransferase (ALCAT1) in mouse. *J. Biol. Chem.* **279:** 31727–31734.
27. Xu, Y., R. I. Kelley, T. J. Blanck, and M. Schlame. 2003. Remodeling of cardiolipin by phospholipid transacylation. *J. Biol. Chem.* **278:** 51380–51385.
28. Pfeiffer, K., V. Gohil, R. A. Stuart, C. Hunte, U. Brandt, M. L. Greenberg, and H. Schagger. 2003. Cardiolipin stabilizes respiratory chain supercomplexes. *J. Biol. Chem.* **278:** 52873–52880.
29. Tuller, G., C. Hrastnik, G. Achleitner, U. Schiefthaler, F. Klein, and G. Daum. 1998. YDL142c encodes cardiolipin synthase (Cls1p) and is non-essential for aerobic growth of *Saccharomyces cerevisiae*. *FEBS Lett.* **421:** 15–18.
30. Zhong, Q., V. M. Gohil, L. Ma, and M. L. Greenberg. 2004. Absence of cardiolipin results in temperature sensitivity, respiratory defects, and mitochondrial DNA instability independent of pet56. *J. Biol. Chem.* **279:** 32294–32300.
31. Mikhaleva, N. I., V. V. Golovastov, S. N. Zolov, M. V. Bogdanov, W. Dowhan, and M. A. Nesmeyanova. 2001. Depletion of phosphatidylethanolamine affects secretion of *Escherichia coli* alkaline phosphatase and its transcriptional expression. *FEBS Lett.* **493:** 85–90.
32. Breitschopf, K., A. M. Zeiher, and S. Dimmeler. 2000. Ubiquitin-mediated degradation of the proapoptotic active form of bid. A functional consequence on apoptosis induction. *J. Biol. Chem.* **275:** 21648–21652.
33. Kuijpers, T. W., N. A. Maianski, A. T. Tool, K. Becker, B. Plecko, F. Valianpour, R. J. Wanders, R. Pereira, J. Van Hove, A. J. Verhoeven, et al. 2004. Neutrophils in Barth syndrome (BTHS) avidly bind annexin-V in the absence of apoptosis. *Blood.* **103:** 3915–3923.